

# Large Scale Fluctuations in the X-Ray Background

Marie Treyer<sup>1</sup>, Caleb Scharf<sup>2</sup>, Ofer Lahav<sup>3</sup>, Keith Jahoda<sup>4</sup>, Elihu Boldt<sup>4</sup>, Tsvi Piran<sup>5</sup>

<sup>1</sup> Astrophysikalisches Institut Potsdam, An der Sternwarte 16, 14842 Potsdam, Germany,  
 mtreyer@aip.de

<sup>2</sup> Space Telescope Science Institute, 3700 San Martin Drive, Baltimore, MD 21218,  
 scharf@stsci.edu

<sup>3</sup> Institute of Astronomy, Madingley Road, Cambridge CB3 OHA, U.K.; lahav@ast.cam.ac.uk

<sup>4</sup> Laboratory for High Energy Astrophysics, NASA/GSFC, Greenbelt, MD 20771,  
 keith@pcasrv2.gsfc.nasa.gov, boldt@lheavx.gsfc.nasa.gov

<sup>5</sup> Racah Institute of Physics, The Hebrew University, Jerusalem 91904, Israel,  
 tsvi@shemesh.fiz.huji.ac.il

## ABSTRACT

We present an attempt to measure the large angular scale fluctuations in the X-Ray Background (XRB) from the HEAO1-A2 data, expressed in terms of spherical harmonics. We model the harmonic coefficients assuming a power spectrum and an epoch-dependent bias parameter,  $b_x(z)$ , and using a phenomenological scenario describing the evolution of the X-ray sources. From the few low-order multipoles detected above shot noise, we estimate the power-spectrum normalization on scales intermediate between those explored by local galaxy redshift surveys ( $\sim 100h^{-1}$  Mpc) and those probed by the COBE Cosmic Microwave Background (CMB) measurements ( $\sim 1000h^{-1}$  Mpc). We find that the HEAO1 harmonics are consistent with present epoch rms fluctuations of the X-ray sources  $b_x(0)\sigma_8 \sim 1 - 2$  in  $8 h^{-1}$  Mpc spheres. Therefore the observed fluctuations in the XRB are roughly as expected from interpolating between the local galaxy surveys and the COBE CMB experiment. We predict that an X-ray all-sky surface brightness survey resolving sources a factor of 10 fainter than HEAO1, may reveal fluctuations to significantly larger scales and therefore more strongly constrain the large scale structure of the Universe on scales of hundreds of Mpc.

*Subject headings:* X-rays: diffuse radiation — cosmology: observations, large-scale structure of universe

## 1. Introduction

Although discovered before the Cosmic Microwave Background (CMB), the origin of the hard X-Ray Background (XRB) is still not fully understood. At energies below 2 keV, the XRB has

now been almost entirely resolved into discrete sources. Most of these are AGN's but other types of sources (e.g. clusters, narrow emission line galaxies) may also contribute a significant fraction of the total flux (Hasinger et al. 1998, McHardy et al. 1998). The X-ray spectra of these sources are, for the most part, too soft to account for the shape and total intensity of the XRB above 2 keV, but absorption can be invoked to remedy this problem and allow the full energy range of the XRB to be nicely fitted by the right mixture of absorbed and unabsorbed AGN's (Comastri et al. 1995). Such models have their limitations, but even if the detailed nature of the hard X-ray sources, and their relation to the soft ones, are not fully understood yet, it is now well established that the dominant part of the hard XRB also arises from the integrated emission of discrete sources. The alternative hypothesis of a cosmic hot gas origin was ruled out by the observation of the undistorted CMB spectrum (see Fabian & Barcons 1992 for review).

In order to account for the total flux of the XRB (local X-ray sources only produce a very small fraction of it), X-ray sources must be found throughout a large enough volume of the universe. This makes them convenient tracers of the mass distribution on scales intermediate between those probed by COBE in the CMB ( $\sim 1000$  Mpc), and those probed by optical and IRAS redshift surveys ( $\sim 100$  Mpc). The CMB fluctuations originate from redshift  $z \sim 1000$  and are due to the Sachs-Wolfe effect on scales larger than a few degrees. On the other hand, the fluctuations in the XRB are due to fluctuations in the space density of X-ray sources which are likely to be distributed at  $z \sim 1 - 5$ . In terms of level of anisotropy, the XRB is also intermediate between the CMB fluctuations ( $\sim 10^{-5}$  on angular scales of degrees) and the galaxy density fluctuations (of the order of unity on scale of  $8 h^{-1}$  Mpc).

In this paper, we attempt a comparison between the hard band (2-10 keV) XRB fluctuations seen in the HEAO1-A2 data and a range of models. We measure the fluctuations in terms of spherical harmonic coefficients, and make predictions for the ensemble average of these coefficients using a formalism presented by Lahav, Piran & Treyer (1997) (hereafter LPT97). For related approaches to measurements of the XRB fluctuations see Boughn, Crittenden & Turok (1998) and Carrera, Barcons & Fabian (1997) and references therein. The data analysis and the theoretical formalism are described in Sections 2 and 3 respectively. Measurements and models are compared in Section 4. We present our conclusions in Section 5. For simplicity, we shall assume an Einstein-de Sitter world geometry ( $\Omega = 1, \Lambda = 0$ ). We write the Hubble constant as  $H_0 = 100 h$  km/s/Mpc.

## 2. The HEAO1-A2 Data Analysis

Details of the HEAO1-A2 data analysis will be described in a complementary paper (Scharf et al., in preparation). This section summarizes the procedure.

We use the A2 counts from the 6 months following day 322 of 1977 in the all-sky survey (c.f. Jahoda 1993). The data were provided in rectangular ecliptic coordinates in approximately

$0.5 \times 0.25$  degree pixels (at ecliptic equator), which considerably oversamples the  $3 \times 1.5$  degree FWHM beam. These data are then corrected for a small systematic instrumental change from day  $\sim 430$  onwards. In this work, we further bin the data into groups of 12 by 12 pixels (smaller resolution pixels are strongly correlated due to the instrument beam) for all analyses. At the ecliptic equator the pixel groups are therefore  $6^\circ \times 3^\circ$ . Masking (see below) is however performed initially on the higher resolution data and the final pixel groups contain the *mean* count rate of all non-zero ‘sub-pixels’ and are weighted according to their area.

It is difficult to unambiguously separate foreground (Galactic) from background (extragalactic) information in the HEAO1 X-ray data. The total number of resolved foreground and background sources ( $|b| > 20^\circ$ ) is small ( $\sim 0.01 \text{ deg}^{-2}$ ) and a detailed model of possible large scale Galactic emission is hard to determine. However, the Galactic 2-10 keV emission model of Iwan et al. (1982) predicts variations of no more than 3% of the total flux due to smoothly distributed emission of Galactic origin at latitudes  $|b| > 20^\circ$ . Studies in the soft bands ( $< 0.75$  keV) by ROSAT (Snowden 1996) indicate that, at these lower energies, the picture is more complicated, with Galactic emission at all scales.

In the present work, as a first step towards removing the foreground, we construct a ‘mask’ using a list of resolved and identified Galactic X-ray sources (Piccinotti et al. 1982) and a  $|b| < 20^\circ$  Galactic Plane mask. Regions of sizes varying from  $\sim 8^\circ$  to  $12^\circ$  diameter are excised around resolved sources, larger regions are removed around the Large and Small Magellanic Clouds. A total of  $\sim 23\%$  of the raw all-sky flux is removed by this ‘Galactic’ mask.

The removal of bright extragalactic sources is also very important in order to control shot-noise in the angular power estimates (LPT97). We attempt to do this by further masking out all 61 extragalactic sources (AGN’s and clusters) in the catalogue of Piccinotti et al. (1982), to a flux limit of  $S_{cut} = 3 \times 10^{-11} \text{ erg s}^{-1} \text{ cm}^{-2}$  (2-10 keV). An additional  $\sim 22\%$  of the raw all-sky flux is removed by this ‘extragalactic’ mask (the combination of large beam and cautiously generous source excision results in  $\sim 50 \text{ deg}^2$  being removed per source). The final unmasked area is therefore  $\sim 55\%$  of the sky with an effective redshift of  $\sim 0.02$  (approximately the median redshift of the Piccinotti et al. sources).

Finally, the dipolar contribution to the anisotropy due to the motion of the observer with respect to the XRB, the Compton-Getting (CG) effect, is subtracted from the flux (Boldt 1987, Jahoda 1993, LPT97). The amplitude of this dipole is estimated from our observed motion with respect to the CMB and the observed spectral index of the hard XRB ( $\alpha = 0.4$ ). We note that the raw HEAO1 dipole (Galactic sources and plane removed), due to both the CG effect and large scale structure (see LPT97), points in the direction  $l \approx 330^\circ; b \approx 33^\circ$ . This can be compared with the CMB dipole (in the Local Group frame) which points towards  $l \approx 268^\circ; b \approx 27^\circ$  (based on COBE, Lineweaver et al. 1996). We shall further discuss the HEAO1 dipole elsewhere (Scharf et al., in preparation). The HEAO1 data are then expanded in spherical harmonics and the harmonic coefficients determined (Scharf et al. 1992, LPT97).

### 3. Modeling

To model the large angular scale fluctuations in the XRB, we follow the formalism proposed by LPT97 using the following new set of assumptions:

(i) X-ray light traces mass, and we assume linear, epoch-*dependent* biasing between the spatial fluctuations in the X-ray source distribution,  $\delta_x$ , and those in the underlying mass distribution,  $\delta_M$ :  $\delta_x(z) = b_x(z)\delta_M(z)$ . We adopt the following prescription (Fry 1996) for the time-dependence of the biasing parameter, which we parametrize in terms of the present-epoch parameter  $b_x(0)$ :

$$b_x(z) = b_x(0) + z[b_x(0) - 1] \quad (1)$$

This assumption is somewhat more realistic than the time-independent bias parameter used by LPT97. In Fry's model the galaxies are formed at an early epoch  $z_*$  in a biased way, then cluster with time under the influence of gravity. Note that if  $b_x(z_*) = 1$  then  $b_x(0) = 1$ . However, if  $b_x(z_*) > 1$ , biasing decreases with cosmic epoch (see also Bagla 1998).

(ii) We assume an Einstein-de Sitter cosmology ( $\Omega = 1, \Lambda = 0$ ), but we use a phenomenological low-density CDM model (with shape parameter  $\Gamma = 0.2$ ) to represent the present-day power-spectrum  $P(k) \equiv \sigma_8^2 \bar{P}(k)$ , where  $\sigma_8$  is the present-epoch normalization of the mass fluctuations in  $8 h^{-1}$  Mpc spheres. In this case the mass power-spectrum evolves according to linear theory as  $P(k, z) \propto (1+z)^{-2}$ . For the X-ray light fluctuations,  $\delta_x(\mathbf{k}, z)$ , the above assumptions translate into:

$$\langle \delta_x(\mathbf{k}) \delta_x^*(\mathbf{k}') \rangle(z) = (2\pi)^3 \sigma_8^2 b_x^2(z) \bar{P}(k) (1+z)^{-2} \delta^{(3)}(\mathbf{k} - \mathbf{k}'), \quad (2)$$

where  $\delta^{(3)}$  is the three-dimensional delta-function.

(iii) The X-ray intensity observed in the 2-10 keV energy band originates from the integrated emission of discrete X-ray sources out to some high redshift  $z_{max}$ . We describe this population by its local luminosity function  $\phi_x(L)$  and spectral index  $\alpha$ , and assume simple power-law evolution both in luminosity:  $L(z) \propto (1+z)^e$ , and in number density:  $\phi(L, z) \propto (1+z)^d$ . The local X-ray light density is:

$$\rho_0 = \int_0^\infty L \phi_x(L) dL, \quad (3)$$

and the X-ray light density at redshift  $z$  *observed* in the 2-10 keV energy range is:

$$\rho_x(z) = \rho_0 (1+z)^q \quad (4)$$

where  $q = d + e - \alpha + 1$ .

We use the above assumptions to predict the ensemble average of the spherical harmonic coefficients in the XRB. The total predicted signal results in a large scale structure component, reflecting the underlying mass distribution, and a shot noise component due to the discreteness of the sources (as opposed to the continuous mass distribution):

$$\langle |a_l^m|^2 \rangle_{model} = \langle |a_l^m|^2 \rangle_{LSS} + \langle |a_l^m|^2 \rangle_{SN}. \quad (5)$$

The shot noise term is:

$$\langle |a_l^m|^2 \rangle_{SN} = \frac{1}{4\pi} \sum_{sources} S_i^2 = \int_0^{S_{cut}} S^2 N(S) dS, \quad (6)$$

where  $N(S)$  is the differential number-flux relation of the X-ray sources. Bright sources (brighter than a suitable flux cutoff  $S_{cut}$ ) must be removed to reduce the shot noise. In turn, removing sources, albeit few and nearby, will also reduce the large scale structure signal. However, as we demonstrate below, the shot noise decreases faster than the signal as more and more sources are removed. In other words, the large scale structure signal-to-noise increases when lowering the flux cutoff.

The large scale structure component can be written as an integral over the power spectrum (LPT97):

$$\langle |a_l^m|^2 \rangle_{LSS} = \frac{(r_H \rho_0)^2}{(2\pi)^3} \int k^2 \bar{P}(k) |\Psi_l(k)|^2 dk, \quad (7)$$

where  $r_H = c/H_0$  is the Hubble radius and the window function  $\Psi_l$  contains the model parameters:

$$\Psi_l(k) = \int_0^{z_{max}} \sigma_8 b_x(z) (1+z)^{q-9/2} j_l(kr_c) W_{cut}(z) dz. \quad (8)$$

The function  $W_{cut}(z)$  accounts for the removal of sources brighter than  $S_{cut}$ :

$$W_{cut}(z) = \frac{1}{\rho_0} \int_0^{L_{cut}(z)} L \phi_x(L) dL, \quad (9)$$

where:

$$L_{cut}(z) = 4\pi r_c^2(z) S_{cut} (1+z)^{\alpha+1-e} \quad (10)$$

and  $r_c(z)$  is the comoving radial distance. For the monopole ( $l = 0$ ), we recover the ‘Olbers integral’:  $A_0 = \langle |a_0^0|^2 \rangle_{LLS}^{1/2} = \bar{I} \sqrt{4\pi}$ , where  $\bar{I}$  is the mean total intensity of the XRB. In a flat universe and for  $q \neq 2.5$ , Eq. 4 implies:

$$\bar{I} = \frac{\rho_0 r_H}{4\pi} \times \frac{(1+z_{max})^{q-2.5} - 1}{q - 2.5}. \quad (11)$$

The higher order multipoles characterize the spatial fluctuations of the XRB on angular scales  $\sim \pi/l$ .

In order to compare model expectations with HEAO1 observations, we further convolve our predictions with the foreground masks described above:

$$\langle |c_l^m|^2 \rangle = \sum_{l'm'} |W_{ll'}^{mm'}|^2 \langle |a_{l'm'}|^2 \rangle, \quad (12)$$

where the  $W_{ll'}^{mm'}$  tensor models the mask (Peebles 1980, Scharf et al. 1992, Baleisis et al. 1998). Finally, the masked harmonics and shot noise are normalized over the monopole. We use the following notation:

$$C_{SN} = \frac{\langle |c_l^m|^2 \rangle_{SN}^{1/2}}{A_0} \quad (13)$$

for the shot noise, and for the full signal:

$$C_l = \frac{(\langle |c_l^m|^2 \rangle_{LSS} + \langle |c_l^m|^2 \rangle_{SN})^{1/2}}{A_0}. \quad (14)$$

#### 4. Constraints on model parameters

The local luminosity function in the 2-10 keV energy band can be fitted by a double power-law function between  $\sim 10^{42}$  and  $10^{48} h^{-2}$  ergs s $^{-1}$  (Grossan 1997, Boyle et al. 1998). The integrated emission of local sources in this range of luminosity is:  $\rho_0 \approx 10^{39} h$  ergs s $^{-1}$ Mpc $^3$ . The total intensity of the 2-10 keV XRB is  $\bar{I} = 5.2 \times 10^{-8}$  ergs s $^{-1}$  cm $^2$  sr $^{-1}$ , and its spectral index is  $\alpha = 0.4$  (Boldt 1987).

Boyle et al. (1998) find evidence for strong cosmological evolution matching a ‘pure’ luminosity evolution model:  $L_x \propto (1+z)^e$  with  $e \approx 2$  out to a redshift of  $\sim 2$ , followed by a declining phase. This scenario would have to hold to  $z_{max} \approx 6.4$  in order to account for the total XRB intensity (Eq. 11), and thus requires other processes or populations whose X-ray emission would add to that currently observed. On the other hand, Hasinger (1998) argues that strong *number* density evolution:  $\phi(L, z) \propto (1+z)^d$  with  $d \approx 4$ , provides a better fit to the ROSAT deep sky survey data, implying that the whole XRB intensity should be accounted for by  $z_{max} \approx 1.3$ . New results from the Hamburg/ESO survey show that QSO’s keep evolving strongly to  $z \sim 3$  and that none of the above simple parameterizations is an acceptable representation of the data (Wisotzki, private communication). For simplicity however, we shall use the following two toy models to bracket more realistic X-ray source evolution scenarios: on the one hand, a ‘pure’ luminosity evolution model with  $q = e - \alpha + 1 = 2.6$  (see Eq. 4) and  $z_{max} = 6.4$ ; on the other hand, a ‘pure’ density evolution model with  $q = d - \alpha + 1 = 4.6$  and  $z_{max} = 1.3$ .

We compute the differential number counts relation for both models. Both are in good agreement with the Euclidean curve,  $N(S) \propto S^{-2.5}$ , derived from ASCA deep sky observations to  $S \sim 5 \times 10^{-14}$  ergs s $^{-1}$ cm $^{-2}$  (e.g. Georgantopoulos et al. 1997). At fainter fluxes both predicted logN-logS relations slightly bend down to  $S \sim 5 \times 10^{-16}$  ergs s $^{-1}$ cm $^{-2}$ , at which flux the total intensity of the XRB is accounted for. From these number counts, we derive the shot noise level as a function of flux cutoff (Eq. 6).

#### 5. Results

Figure 1 shows the normalized HEAO1 XRB harmonics measured through the ‘Galactic’ mask (upper panel) and through the full, foreground removed mask (lower panel) respectively. The lower shot noise from bright source removal is immediately apparent as a lowering in the overall harmonic amplitude. The various lines represent our model predictions for the shot noise and large scale structure signal, as described below.

Both evolution scenarios yield similar shot noise values within 5%. Masking induces the otherwise constant shot noise to decrease slightly (by less than 10%) towards the high  $l$ 's. As the difference between the two evolution scenarios and the gradient due to masking are negligible, we have plotted the mean shot noise value as one horizontal line on both panels in Fig. 1: for  $S_{cut} = 3 \times 10^{-10} \text{ ergs s}^{-1} \text{ cm}^{-2}$  (i.e. Galactic sources removed),  $C_{SN} \approx 1.1 \times 10^{-3}$ ; for  $S_{cut} = 3 \times 10^{-11} \text{ ergs s}^{-1} \text{ cm}^{-2}$  (i.e. the flux limit of the Piccinotti et al. 1982 catalogue),  $C_{SN} \approx 5.2 \times 10^{-4}$ . The predicted shot noise levels (masked and normalized) are in very good agreement with the flattening of the measured signal in both cases. We verified this by Maximum Likelihood analysis over the harmonic range  $10 \leq l \leq 20$ , ignoring the clustering term and leaving the shot-noise level as a free parameter. We find that the derived shot-noise for both masks is within 10 % of the one predicted from the counts. We also attempted a Maximum Likelihood over the range  $1 \leq l \leq 20$  with 2 free parameters:  $b_x(0)$  and the shot noise level  $C_{SN}$ , but the 2 parameters are strongly coupled. As another independent measure of the shot-noise level we have generated a ‘noise’ map, randomly drawing fluxes out of the real flux distribution using the  $S_{cut} = 3 \times 10^{-11}$  data (i.e. with both Galactic and extragalactic sources from the Piccinotti et al. catalogue removed; The expected CG effect is also removed, as described previously). The noise map is then masked as in the data and the  $C_l$ 's determined. The ‘ $1-\sigma$ ’ errors on the mean over 100 realisations is in excellent agreement with our shot noise estimate independently derived from the source counts (Eq 6).

The first harmonics,  $l = 1 - 3$ , are well above the shot-noise level on both panels, but higher order harmonics are just over  $1-\sigma$  away from the ‘noise’ estimate. (Note that the harmonic measurements are not independent, due to ‘cross talk’ introduced by the mask.) Although contamination from Galactic emission or masking may be non-negligible, it is nevertheless encouraging that the shape of the harmonic spectrum over all  $l$ 's is qualitatively in agreement with the prediction of an extragalactic clustering signal.

All models for the spherical harmonic spectrum plotted in Fig. 1 assume a low density CDM model with shape parameter  $\Gamma = 0.2$  and normalization  $\sigma_8 = 1.0$ . The present-epoch bias parameter  $b_x(0)$  (Eq. 1) was left as a free parameter and its optimal value derived from Maximum Likelihood over the range  $1 \leq l \leq 10$  (neglecting the mask, cf. Scharf et al. 1992). Both evolution scenarios yield the same best fit values:  $b_x(0) = 1.6$  for the Galactic mask, and  $b_x(0) = 1.0$  for the full mask. To illustrate our estimate range, predictions are plotted for these 2 values on *both* panels (Galactic mask and full mask): upper lines are for  $b_x(0) = 1.6$  and lower lines for  $b_x(0) = 1.0$ . The dotted lines represent the density evolution scenario ( $q = 4.6$ ) and the long-dashed lines show the luminosity evolution scenario ( $q = 2.6$ ). Assuming a standard CDM power spectrum yield  $b_x(0) = 1.8$  and 1.2 for Galactic and full masks, respectively. This is not surprising, as low density CDM has more power on large scales than standard CDM.

For most of the models considered above, the reduced  $\chi^2$  is near unity, suggesting acceptable fits. However, the measured multipoles do show more curvature as a function of  $l$  than our models predict. This may be explained by a number of reasons: the low order multipoles measured in the

XRB may result from local (Galactic?) structures unaccounted for by the masks; source clustering evolution may be significantly stronger than the linear theory assumption we have made; or else, the evolution parameters we have used for the X-ray source population are overestimated, at least on part of the redshift range. Note also that the  $b_x(0) = 1$  models, which correspond to constant biasing (see Eq. 1), are flatter than the epoch-dependent biasing models. Therefore we expect stronger bias evolution to improve the fit to the data.

Figure 2 shows the signal-to-noise as a function of  $l$ , assuming  $b_x(0) = 1$  and  $\sigma_8 = 1$  (for the purpose of illustration). In order to compare the above models with predictions at fainter flux limits, we do not use the existing masks. In the lower two panels, we show the signal-to-noise expected if sources brighter than  $S_{cut} = 3 \times 10^{-12}$  and  $3 \times 10^{-13}$  ergs  $s^{-1} cm^{-2}$  respectively (i.e. 1 and 2 magnitudes lower than the present data) could be removed from the X-ray all-sky survey. We predict the signal-to-noise to increase as  $S_{cut}$  decreases. The multipoles are also expected to be detectable above shot noise for an increasing range of  $l$ . As the present results suggest  $b_x(0) \geq 1$ , the signal-to-noise ratios plotted here may be taken as lower limits. Luminosity evolution and density evolution become increasingly distinct as we remove fainter and fainter sources. If sources evolve in luminosity, a given flux cutoff will span a larger redshift range than if they don't or if they only evolve in number, and therefore a larger volume of space will be excluded from the analysis. Hence a weaker signal-to-noise in the case of luminosity evolution than in the case of density evolution. We conclude that an X-ray all-sky survey in the hard band (to minimize Galactic contamination) resolving sources only one magnitude fainter than HEAO1, is likely to reveal large scale fluctuations in the background to significantly higher order than the current data.

Figure 3 shows the amplitude of rms fluctuations,  $(\frac{\delta\rho}{\rho})^2 \sim k^3 P(k)$ , derived at the effective scale  $k^{-1} \sim 600h^{-1}$  Mpc probed by the XRB quadrupole (cf. LPT97 Figure 1). For Galactic mask and either evolution models we find  $\sigma_8 b_x(0) \sim 1.8$  and  $1.6$  for standard and low density CDM models, respectively (marked by the top and bottom crosses). The fractional error on the XRB amplitudes (due to the shot-noise of the X-ray sources) is about 30%. We see that the observed fluctuations in the XRB are roughly as expected from interpolating between the local galaxy surveys and the COBE CMB experiment. The rms fluctuations  $\frac{\delta\rho}{\rho}$  on a scale of  $\sim 600h^{-1}$  Mpc are less than 0.2 %. Our estimate of the fluctuations amplitude derived from HEAO1 is used elsewhere (Wu, Lahav & Rees 1998) to show that the fractal dimension of the universe is very close to 3 (to within  $10^{-4}$ ) on the very large scales. This XRB measurement strongly supports the validity of the Cosmological Principle (Peebles 1993).

## 6. Discussion

We report on the possible detection of low-order spherical harmonic modes in the HEAO1 XRB map. Although one must be cautious about the interpretation of the signal as being purely extragalactic, it is encouraging that the measurements are in agreement with *a priori* predictions.

We find that the XRB fluctuations on scales of a few hundred Mpc are consistent with the result of interpolating between fluctuations derived from local galaxy surveys and those derived from the COBE CMB measurements.

Various models for the matter density fluctuations and the evolution of X-ray sources yield present-epoch biasing factor of typically  $b_x(0) \sim 1 - 2$ . The present analysis allows for epoch-dependent biasing, which seems to give a more reasonable fit than a time-independent biasing model, although both schemes yield similar values of  $b_x(0)$ . Regarding models of density fluctuations, as expected the low density CDM model requires lower  $b_x(0)$  than standard CDM, which has less power on large scales. We note that our values for the local bias factor  $b_x(0)$  are smaller than those derived from the dipole anisotropy of the local AGN distribution (Miyaji 1994) and from HEAO1 assuming epoch-independent biasing (Boughn et al. 1998). On the other hand, our results are in rough agreement with Carrera, Fabian & Barcons (1997) who also find small values of  $b_x(0)$ , although using quite different techniques and data sets, and assuming epoch-independent biasing.

We predict that an X-ray all-sky survey resolving sources a factor of 10 fainter than HEAO1, may allow us to measure large scale fluctuations in the XRB to order  $l \sim 20$  ( $\theta \sim \pi/20$ ). The present data cannot be used with lower flux thresholds as our method of eliminating sources also reduces sky coverage. There are two experimental approaches which can allow a similar analysis to be done while employing a lower flux threshold, thus reducing the shot noise, and allowing a significant measurement of large scale structure over a larger range of  $l$  values.

Barcons et al. (1997) propose an experimental concept that maps the X-ray sky with a collimated proportional counter, substantially similar to the A2 experiment, but with a smaller field of view. Such an experiment can mask individual sources with a smaller penalty in terms of sky coverage (and signal) and can therefore mask a larger number, reaching a fainter limiting flux. But it cannot identify sources an order of magnitude fainter than our flux threshold by itself, and therefore would rely on an externally generated catalogue such as that produced by the ABRIXAS survey (Trümper et al. 1998). The advantages of this approach are the relatively small size and simplicity of the experiment. The combination of ABRIXAS with the experiment proposed by Barcons et al. (1997) can eliminate sources down to a flux threshold  $\sim 1 \times 10^{-12} \text{ erg sec}^{-1} \text{ cm}^{-2}$ . For the expected density of sources (0.3 per square degree) and solid angle of the beam for this experiment (1 square degree), the fraction of the sky that will be masked is comparable to the analysis presented here. This experiment represents the limiting capability of a non focussing mission. The time required to obtain a certain precision per pixel scales inversely with solid angle of the beam, and the fraction of the sky which is masked out remains large.

Removing sources at fainter thresholds requires an imaging experiment capable of identifying, and excluding, faint sources without removing an entire square degree of sky coverage. Due to the relative inefficiency of X-ray telescopes (the effective area is typically  $\leq 25\%$  of the geometric collecting area above 2 keV (Serlemitsos & Soong 1996)) a large collecting area (i.e. many

telescopes) is required to obtain the same precision in the measurement of surface brightness. A collection of imaging telescopes capable of measuring surface brightness to 1% per square degree requires nearly 3 times the geometric collecting area of the proportional counter experiment, but is plausibly within the constraints of NASA Medium Explorer mission (Jahoda 1998). An additional advantage of an imaging experiment is the simultaneous production of a catalogue of sources, useful in their own right as tracers of large scale structure. An experiment capable of identifying sources as faint as  $3 \times 10^{-13}$  erg cm $^{-2}$  sec $^{-1}$  in the 2-10 keV band would generate an all-sky catalogue with  $\geq 10^5$  hard X-ray selected sources.

However ‘old’ and not optimally suited for this analysis, the current data have allowed us to demonstrate that future X-ray missions stand a good chance of revealing significant structure in the matter distribution. Not only are we likely to finally understand the long sought for sources of the hard X-ray background in the coming years, but we may also be able to get a strong hold on the underlying matter distribution in an otherwise little explored range of scales.

The authors thank B. Boyle, M. Rees and K. Wu for helpful discussions. We thank the referee, D. Helfand, for a careful reading and constructive suggestions that have improved this paper.

## REFERENCES

Bagla, J. 1998, MNRAS 297, 251.  
Baleisis, A., Lahav, O., Loan, A. & Wall, J.V. 1998, MNRAS, 297, 545  
Barcons, X., Fabian, A.C., Carrera, F. 1997, MNRAS 285, 820.  
Baugh, C. M. & Efstathiou, G. 1993, MNRAS 265, 145.  
Baugh, C. M. & Efstathiou, G. 1994, MNRAS 267, 323.  
Bennett, C. L. et al. 1996, ApJ 464, L1.  
Boldt, E. A. 1987, Phys. Reports 146, 215.  
Boughn, S., Crittenden, R. & Turok, N. 1998, New Astronomy, vol. 3, no. 5, p. 275.  
Boyle, B.J., Georgantopoulos, I., Blair, A.J., Stewart, G.C., Griffiths, R.E., Shanks, T., Gunn, K.F., Almaini, O. 1998, MNRAS 296, 1.  
Carrera, F., Barcons, X., Fabian, A.C. 1997, MNRAS 285, 820.  
Comastri, A., Setti, G., Zamorani, G., Hasinger, G. 1995, A&A 296, 1.  
Fabian, A. C., Barcons, X. 1992, ARA&A, 30, 429.  
Fry, J. 1996, ApJ, 461, L65.  
Gawiser, E. & Silk, J., 1998, Science, 280, 1405

Georgantopoulos, I., Stewart, G., Blair, A., Shanks, T., Griffiths, R.E., Boyle, B., Almaini, O., Roche, N. 1997, MNRAS 291, 203.

Grossan, B.A. 1992, Ph.D. thesis, MIT.

Hasinger, G. 1998, Astron. Nachr 319, 37.

Hasinger, G., Burg, R., Giacconi, R., Schmidt, M., Trümper, J., Zamorani, G. 1998, A&A, 329, 482.

Iwan, D., Shafer, R.A., Marshall, F.E., Boldt, E.A., Mushotzky, R.F., Stottlemeyer, A. 1982, ApJ, 260, 111.

Jahoda, K. 1993, Adv. Space Res. 13, (12) 231.

Jahoda, K. 1998, Astron. Nachrichten, 319, 129.

Lahav, O., Piran, T., Treyer, M. A. 1997, MNRAS, 284, 499 (LPT97).

Lineweaver, C., Tenorio, L., Smoot, G., Keegstra, P., Banday, A., Lubin, P. 1996, ApJ, 470, 38.

McHardy, I. et al. 1998, Astron. Nachrichten, 319, 51.

Miyaji, T. 1994. PhD thesis, University of Maryland.

Peebles, P.J.E. 1980, Large Scale Structure of the Universe (Princeton University Press).

Peebles, P.J.E. 1993, Principles of Physical Cosmology (Princeton University Press).

Piccinotti, G., Mushotzky, R. F., Boldt, E. A., Holt, S. S., Marshall, F. E., Serlemitsos, P. J., Shafer, R. A. 1982, ApJ, 253, 485.

Scharf, C. A., Hoffman, Y., Lahav, O., Lynden-Bell, D. 1992, MNRAS, 256, 229.

Serlemitsos, P.J., & Soong, Y. 1996, Astrophysics and Space Science, 239, 177.

Snowden, S. L. 1996, in Röntgenstrahlung from the Universe, eds. Zimmermann, H.U., Trümper, J., and Yorke, H., MPE Report 263, 299.

Smoot G., et al., 1992, ApJ L, 396, L1.

Trümper, J., Hasinger, G., & Staubert, R. 1998, Astron. Nachrichten, 319, 113.

Wu, K.K.S., Lahav, O. & Rees, M.J., 1998, submitted to Nature (astro-ph/9804062)

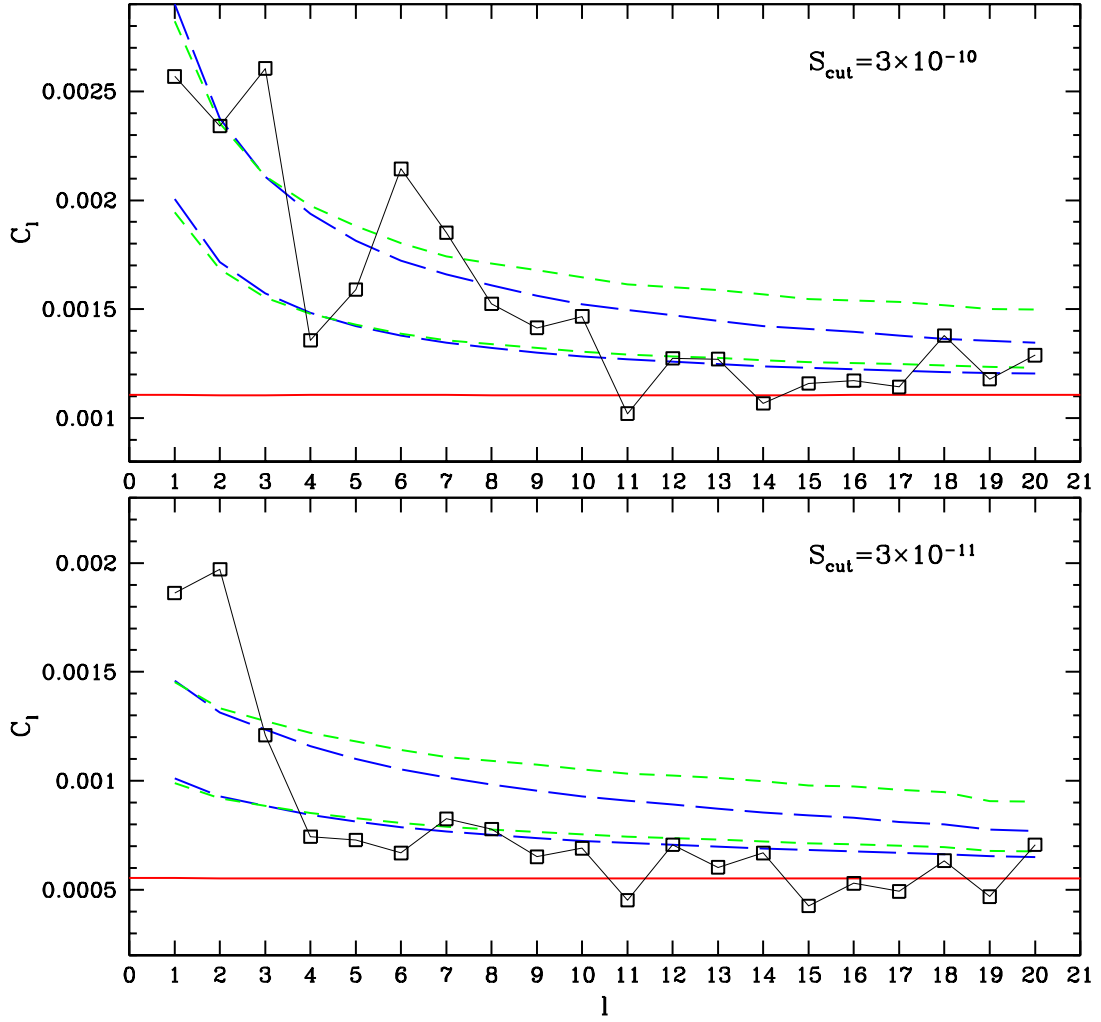


Fig. 1.— The normalized spherical harmonic spectrum of the HEAO1 XRB (squares). In the upper panel, only the Galactic component was removed from the data. In the lower panel, extragalactic X-ray sources from the Piccinotti et al. 1982 catalogue were also removed. The corresponding flux cutoffs  $S_{cut}$  in  $\text{ergs s}^{-1}\text{cm}^{-2}$  and predicted levels of shot noise (horizontal lines) are indicated in both cases. The dotted lines are the predictions (Eq. 5) of a ‘pure’ density evolution model ( $q = 4.6$ ), and the long-dashed lines are the predictions of a ‘pure’ luminosity evolution model ( $q = 2.6$ ). A low density CDM power-spectrum with normalization  $\sigma_8 = 1$  for the mass fluctuations was assumed. Upper lines on both panels are for present-epoch bias parameter  $b_x(0) = 1.6$  and lower lines for  $b_x(0) = 1.0$ .

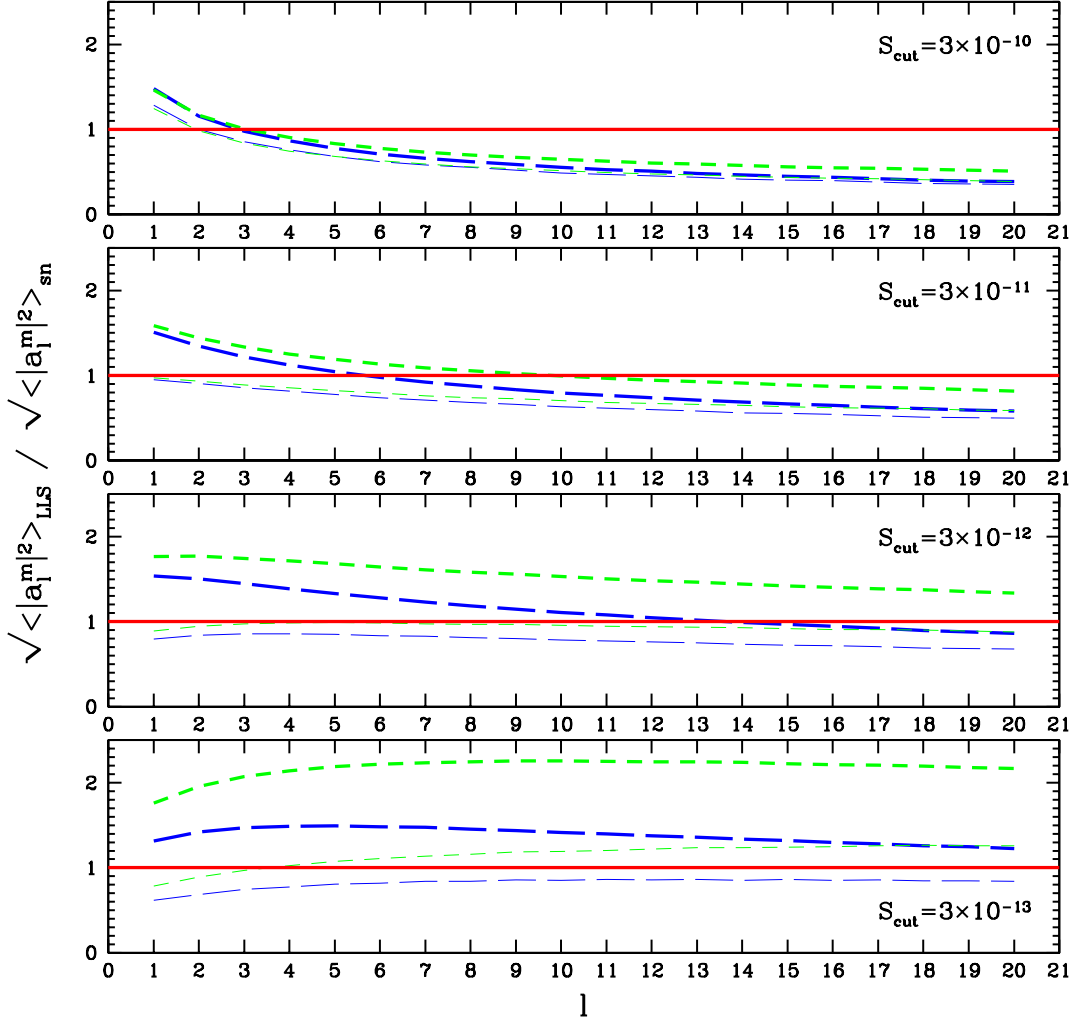


Fig. 2.— Predicted signal-to-noise as a function of  $l$  for decreasing flux cutoffs  $S_{\text{cut}}$  (as indicated on each panel in  $\text{ergs s}^{-1}\text{cm}^{-2}$ ). We assumed  $b_x(0) = 1$  and  $\sigma_8=1$ . The dotted lines are the predictions of a ‘pure’ density evolution model ( $q = 4.6$ ), and the long-dashed lines are the predictions of a ‘pure’ luminosity evolution model ( $q = 2.6$ ). The thick lines assume a low density CDM power spectrum as described in the text. The thinner lines correspond to a standard CDM power-spectrum, for comparison. The horizontal line (signal/noise = 1) marks the shot-noise level (also the  $1-\sigma$  error bar).

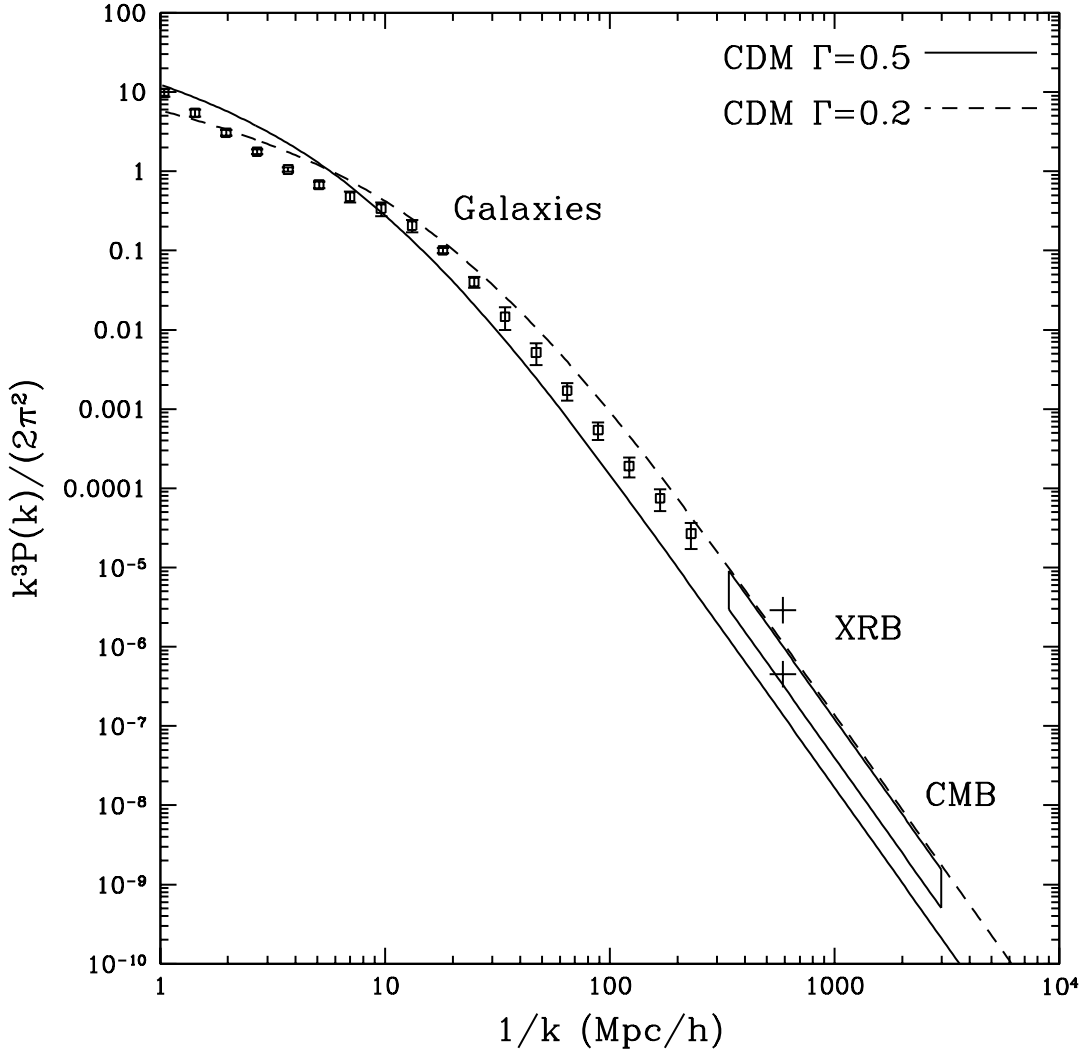


Fig. 3.— A compilation of rms density fluctuations,  $(\frac{\delta\rho}{\rho})^2 \sim k^3 P(k)$ , on different scales from various observations: a galaxy survey, the X-ray Background and Cosmic Microwave Background experiments. The crosses represent our present constraints from the XRB HEAO1 quadrupole. The top and bottom crosses are estimates of the amplitude of the power-spectrum at  $k^{-1} \sim 600h^{-1}$  Mpc, assuming CDM power-spectra with shape parameters  $\Gamma = 0.2$  and  $0.5$  respectively, and an Einstein-de Sitter universe. The fractional error on the XRB amplitudes (due to the shot-noise of the X-ray sources) is about 30%. The solid and dashed lines correspond to the standard CDM power-spectrum (with shape parameter  $\Gamma = 0.5$ ) and a ‘low-density’ CDM power-spectrum (with  $\Gamma = 0.2$ ), respectively, assuming  $\sigma_8 = 1$  in both cases. The open squares at small scales are estimates of the power-spectrum from 3D inversion of the angular APM galaxy catalogue (Baugh & Efstathiou 1993, 1994). The elongated box at large scales represent the COBE 4-yr CMB measurement (Smoot et al. 1992, Bennett et al. 1996). The COBE box corresponds to a quadrupole  $Q=18.0 \mu K$  for a Harrison-Zeldovich mass power-spectrum, via the Sachs-Wolfe effect, or  $\sigma_8 = 1.4$  for a standard CDM model (Gawiser and Silk 1998).